Scientia Iranica B (2014) 21(2), 403–413

SCIENTIA IRANICA

Sharif University of Technology
Scientia Iranica
Transactions B: Mechanical Engineering
www.scientiairanica.com

Effects of micro-structural parameters on mechanical properties of carbon nanotube polymer nanocomposites

E. Bafekrpour[a,b], M. Salehi[b,*], E. Sonbolestan[c] and B. Fox[a]

a. *Institute for Frontier Materials, Deakin University, Locked Bag 20000, Geelong, Victoria 3220, Australia.*
b. *Department of Mechanical Engineering and Centre of Excellence in Smart Structures and Dynamical Systems, Amirkabir University of Technology, Hafez Ave., Tehran, P.O. Box 1591634311, Iran.*
c. *Department of Mechanical Engineering, Iran University of Science and Technology, Tehran, P.O. Box 16846-13114, Iran.*

Received 16 September 2012; received in revised form 29 June 2013; accepted 21 September 2013

KEYWORDS
Micromechanics models;
Finite Element Modeling (FEM);
Nanocomposite;
Carbon nanotube;
Mechanical properties.

Abstract. A comparison between the elastic modulus of carbon nanotube (CNT) polymer nano composites predicted by classical micromechanics theories, based on continuum mechanics and experimental data, was made and the results revealed a great difference. To improve the accuracy of these models, a new two-step semi-analytical method was developed, which allowed consideration of the effect of the interphase, in addition to CNT and matrix, in the modeling of nanocomposites. Based on this developed method, the influence of microstructural parameters, such as CNT volume fraction, CNT aspect ratio, partial and complete agglomerations of CNTs, and overlap and exfoliation of CNTs, on the overall elastic modulus of nanocomposites was investigated.

1. Introduction

The exceptional properties of CNTs make them a very promising reinforcement for advanced nanocomposites [1,2]. To fully take advantage of this potential, many parameters such as CNT distribution and interfacial effects need to be investigated to obtain an optimized design of CNT nanocomposites. However, it is extremely difficult to experimentally study the effects of interphase on the overall mechanical properties of nanocomposites. Numerical and analytical methods of modeling nanocomposites have become a hot topic. The mechanical behavior of CNT/polymer nanocomposites is investigated using Molecular Dynamics (MD) simulation [3,4], shear-lag method [5], and Finite Element Modeling (FEM). MD simulations suffer from complex formulations and great amounts of computational effort. FEM is very effective in resolving complex engineering problems and more suitable for large scale systems such as nanocomposites. Mechanical and thermoelastic properties of CNT/polymer nanocomposites were extensively investigated using FEM [6-8]. The effects of parameters such as CNT geometry and distribution patterns on the different behavior of nanocomposites were also investigated [9-15]. However, FEM formulation is based on classical mechanics, which do not encounter atomic interactions and quantum effects between CNT and the polymer matrix.

An equivalent continuum modeling method was developed to consider the influence of interphase on the properties of the nanocomposites [16,17]. Shokrieh and Rafiee [18,19], for example, used a non-linear analysis on a full 3D multi-scale finite element model consisting of CNT, a non-bonded interphase region and a surrounding polymer to study the longitudinal behavior of a carbon nanotube in a polymeric matrix. Yang et al. [20] presented a hierarchical multiscale modeling approach to characterize the elastic and plastic behavior of nanocomposites via molecular dynamics

*. *Corresponding author. Tel.: +98 (21) 645 43447; Fax: +98(21) 66419736*
E-mail address: msalehi@aut.ac.ir (M. Salehi)

simulations and continuum nonlinear micromechanics, based on the secant moduli method.

Classical micromechanics theories, including the dilute Eshel by model [21], the Mori-Tanaka model [22], Self-consistent models [23,24], and the Halpin-Tsai [25] model, are also widely used to model composites with reinforcements at micro-scale or higher levels [26]. Li et al. [27] used micromechanical models to study the visco-elastic properties of carbon nanotube-reinforced polymer composites. However, the accuracy of these methods is not examined for CNT/polymer nanocomposites in which the reinforcement is at the scale of nano. Moreover, it is experimentally shown that the dispersion and agglomeration of CNTs within the matrix have significant effects on the overall mechanical properties of the nanocomposites [28,29]. However, to the best of the author's knowledge, no theoretical model has been reported to analyze the micro-structural parameters, such as agglomeration, overlap and exfoliation of CNTs in the matrix, considering the effect of interphase properties.

In the present work, the mechanical properties of CNT/polymer nanocomposites were modeled using classical continuum-based micromechanics theories and the results were compared with experimental results. It was concluded that these models cannot predict the mechanical behavior of composites with nano-scale reinforcements accurately. A two-step method was presented to develop classical micromechanics theories in order to consider the effect of CNT/polymer interphase on the mechanical properties of nanocomposites. The effect of micro-structural parameters, including agglomeration, overlap and exfoliation of CNTs, on the mechanical properties of nanocomposites was studied using the developed micromechanics theories.

2. Theoretical modeling of CNT/polymer nanocomposites using micromechanics theories

The average composite stiffness in terms of the strain-concentration tensor, CNT and matrix properties can be expressed as [26]:

$$C = C^m + \nu_{\rm CNT}\left(C^{\rm CNT} - C^m\right)A, \tag{1}$$

where c and $C^{\rm CNT}$ are the polymer and CNT stiffness matrix, $\nu_{\rm CNT}$ is the volume fraction of CNT and A is the fourth-order strain-concentration tensor, which was defined by solving the microscopic stress and strain fields. However, different micromechanics theories, based on Eshelby's equivalent inclusion, suggest different ways to approximate the strain-concentration tensor, A, for aligned fiber composites. The strain concentration tensor for Eshelby's equivalent inclusion is given as [26]:

$$A^{\rm Eshelby} = \left[I + HS^m\left(C^{\rm CNT} - C^m\right)\right]^{-1}, \tag{2}$$

where H is Eshelby's tensor which is given in the Appendix.

The strain concentration tensor according to the Mori-Tanaka theory is given by:

$$A^{MT} = A^{\rm Eshelby}\left[(1-\nu_{\rm CNT})I + \nu_{\rm CNT}A^{\rm Eshelby}\right]^{-1}, \tag{3}$$

and, according to the self-consistent model, by:

$$A^{SC} = \left[I + HS^m\left(C^{\rm CNT} - C\right)\right]^{-1}. \tag{4}$$

In the self-consistent method, a primary estimation for overall composite properties is considered in Eq. (4), and A^{SC} is calculated. Then, composite stiffness is calculated using Eq. (1) to achieve an enhanced value for approximation of C. The process is repeated until the results for the overall composite stiffness converge. The composite stiffness according to the Bounding model is [30]:

$$C = \left[\nu_{\rm CNT}C^{\rm CNT}Q^{\rm CNT} + \nu_m C^m Q^m\right] \left[\nu_{\rm CNT}Q^{\rm CNT} + \nu_m Q^m\right]^{-1}, \tag{5}$$

where the tensors, $Q^{\rm CNT}$ and Q^m, are defined as:

$$Q^{\rm CNT} = \left[I + H^R S^R\left(C^{\rm CNT} - C^R\right)\right]^{-1}, \tag{6}$$

$$Q^m = \left[I + H^R S^R\left(C^m - C^R\right)\right]^{-1}, \tag{7}$$

and H^R is Eshelby's tensor related to the properties of the reference material with stiffness C^R and compliance S^R. The lower bound of composite stiffness can be analyzed by considering the matrix as the reference material:

$$A^{\rm Lower} = \left[I + H^m S^m\left(C^{\rm CNT} - C^m\right)\right]^{-1}. \tag{8}$$

The upper bound of composite stiffness can be examined by considering the CNT as the reference material:

$$A^{\rm Upper} = \left[I + H^{\rm CNT}S^{\rm CNT}\left(C^m - C^{\rm CNT}\right)\right]. \tag{9}$$

Halpin-Tsai equations for prediction of composite stiff-

ness is [31]:

$$\frac{P}{P_m} = \frac{1 + \xi\eta\nu_{\mathrm{CNT}}}{1 - \eta\nu_{\mathrm{CNT}}}, \tag{10}$$

where $\eta = \frac{(P_{\mathrm{CNT}}/P_m)-1}{(P_{\mathrm{CNT}}/P_m)+\xi}$, and P represents E_{11} and E_{22} of the composite. P_{CNT} and P_m are the moduli of the CNT and matrix, respectively.

The composite stiffness according to the Voigt model, which supposes the same uniform strain for CNT and matrix, can be calculated as:

$$C^{\mathrm{Voigt}} = C^m + \nu_{\mathrm{CNT}}\left(C^{\mathrm{CNT}} - C^m\right)$$

$$= \nu_{\mathrm{CNT}}C^{\mathrm{CNT}} + \nu_m C^m. \tag{11}$$

However, the Reuss model, in which the same uniform stress is assumed for both CNT and matrix, predicts the compliance of the composite as:

$$S^{\mathrm{Reuss}} = S^m + \nu_{\mathrm{CNT}}\left(S^{\mathrm{CNT}} - S^m\right)$$

$$= \nu_{\mathrm{CNT}}S^{\mathrm{CNT}} + \nu_m S^m. \tag{12}$$

In order to model a nanocomposite with randomly oriented CNTs using micromechanics theories, the average strain concentration tensor should be calculated as [16]:

$$\overline{A}_{ijkl} = c_{ip}c_{jq}c_{kr}c_{ls}A_{pqrs}, \tag{13}$$

where c_{ij} is the direction cosine for the transformation from the local CNT coordinates $(o-xyz)$ to the global coordinates $(o-XYZ)$, as schematically presented in Figure 1 $(i,j,k,l,p,q,k,s = 1,2,3)$.

$$c_{11} = \cos\phi\cos\psi - \sin\phi\cos\gamma\sin\psi,$$

$$c_{12} = \sin\phi\cos\psi - \cos\phi\cos\gamma\sin\psi,$$

$$c_{13} = \sin\psi, \sin\gamma,$$

$$c_{21} = -\cos\phi\sin\psi - \sin\phi\cos\gamma\cos\psi,$$

$$c_{22} = -\sin\phi\sin\psi + \cos\phi\cos\gamma\cos\psi,$$

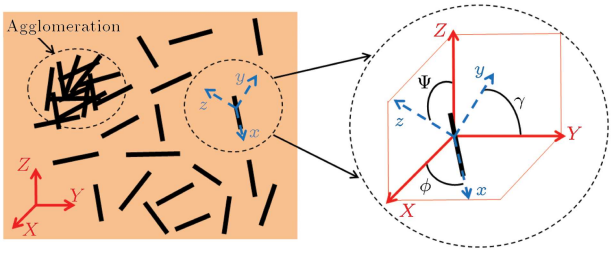

Figure 1. Inclusion model of agglomeration of randomly oriented CNTs and their orientation angles.

$$c_{23} = \sin\gamma\cos\psi,$$

$$c_{31} = \sin\phi\cos\gamma,$$

$$c_{32} = -\cos\phi\cos\gamma,$$

$$c_{32} = \cos\gamma. \tag{14}$$

The orientation average of the strain concentration tensor can be calculated as [32]:

$$A = \frac{\int_{-\pi}^{\pi}\int_{0}^{\pi}\int_{0}^{\pi/2}\bar{A}(\phi,\gamma,\psi)\lambda(\phi.\gamma)sin(\gamma)d\phi d\gamma d\psi}{\int_{-\pi}^{\pi}\int_{0}^{\pi}\int_{0}^{\pi/2}\lambda(\phi,\psi)sin(\gamma)d\phi d\gamma d\psi}, \tag{15}$$

where $\lambda(\phi,\psi)$ is the orientation distribution function and is expressed as:

$$\lambda(\phi,\psi) = \exp\left(-b_1\phi^2\right)\exp\left(-b_2\psi^2\right), \tag{16}$$

where b_1 and b_2 are factors that control the orientation. The distribution of the CNTs is completely random when $b_1 = b_2 = 0$.

3. Developing interphase model for micromechanics theories

In the micromechanics models, it is assumed that only two phases exist: matrix and reinforcement. These theories have shown perfect prediction of overall properties of composites with reinforcement at micro-scale or higher, because, at these scales, the assumption of the existence of two phases is acceptable. However, in case of reinforcement at nano-scale, it has been shown that the molecular structure of the polymer matrix is changed at the interface of the reinforcement and polymer, due to interaction between the polymer molecules and the surface of the CNT [33]. This interphase is on the same scale as the nano-scale reinforcement [16,34,35]. Therefore, in addition to nano-scale reinforcement and the polymer matrix, there is another phase, not considered in micromechanical models, which, in turn, decreases the accuracy of the theoretical prediction of nanocomposite stiffness. Many models have been developed to consider this interphase in the modeling of nanocomposites [18,19,36,37]. However, in this study we developed a semi-analytical modeling approach to predict the elastic properties of composites with nano-scale reinforcement considering the interphase effect. In this model, the interphase was considered a continuous and homogeneous region around the CNT with a finite size and perfectly bonded to the CNT and polymer matrix.

The assumption of material continuity is necessary to develop constitutive relations based on continuum micromechanics. The interphase was considered as a cylinder around the CNT, with linear elastic

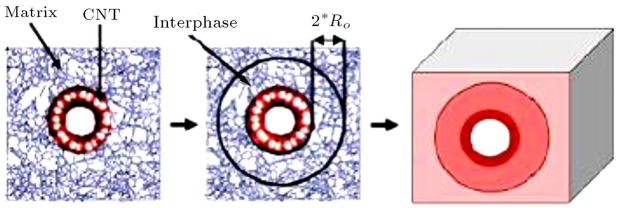

Figure 2. Schematic of the process used to determine the effective interphase.

behavior, with a thickness of two times the radius of CNT. The properties of this interphase are unknown for modeling the nanocomposite. The interphase was simply considered to be isotropic. Therefore, two constants are necessary to describe the elastic behavior of the interphase. For simplicity, the Poisson ratio of the interphase was considered the same as the Poisson ratio of the polymer matrix (it should be noted that the Poisson ratio of the interphase may be different from the polymer matrix and may introduce some error in the model). The CNT and the adjacent interphase were considered as a composite inclusion, in which the CNT was considered as reinforcement, and the interphase considered as its matrix with unknown properties. Then, this composite inclusion (containing CNT and interphase) was considered reinforcement for the polymer matrix. The scheme in Figure 2 shows how this interphase region was defined.

In each theory, first, a primary guess was made for the elastic modulus of interphase. Then the properties of the inclusion, consisting of CNT and interphase, were determined and, in the next step, the elastic modulus of the nanocomposite was calculated by considering this inclusion as reinforcement for the polymer matrix. This calculated value for the elastic modulus of the nanocomposite was compared with the experimental data and the primary guess was evaluated until the predicted modulus for the nanocomposite matched the experimental data.

The elastic properties of the interphase were determined according to each micromechanics theory and used for exact prediction of the nanocomposite and for studying the effect of microstructural parameters on the mechanical properties of the nanocomposite. As the experimental data is required to find Young's modulus of the interphase using the iterative estimation method, it is considered a semi-analytical approach.

4. Effect of microstructural parameters on mechanical properties of the nanocomposite

4.1. Agglomeration of CNTs

Hitherto, it was assumed that CNTs were uniformly dispersed in the matrix. However, it has been observed that the distribution of CNTs in the matrix is not uniform and a large amount of CNTs is concentrated in aggregates [38-43]. Since the classical micromechanics models based on continuum mechanics do not take into account the effect of agglomeration, an analytical model was applied to study the effect of agglomeration of CNTs on the effective elastic moduli of CNT/polymer nanocomposites. In order to study the effect of agglomeration on the elastic modulus, the Mori-Tanaka method, based on the presented interphase model, was used. The regions with concentrated CNTs were assumed to have spherical shapes, and were considered inclusions, as shown in Figure 2.

The total volume, $V_{\rm CNT}$, of CNTs in the Representative Volume Element (RVE) can be divided into the following two parts [29]:

$$V_{\rm CNT} = V_{\rm CNT}^{\rm inclusion} + V_{\rm CNT}^{m}, \tag{17}$$

where $V_{\rm CNT}^{\rm inclusion}$ and $V_{\rm CNT}^{m}$ indicate the volumes of CNTs dispersed in the inclusions (concentrated regions) and in the matrix, respectively. Two parameters, α and β, were introduced to describe the agglomeration of CNTs:

$$\alpha = \frac{V_{\rm inclusion}}{V}, \quad \beta = \frac{V_{\rm CNT}^{\rm inclusion}}{V_{\rm CNT}}, \tag{18}$$

where $V_{\rm inclusion}$ is the volume of the sphere inclusions in the RVE and α denotes the volume fraction of inclusions with respect to the total volume, V, of the RVE. When $\alpha = 1$, CNTs are uniformly dispersed in the matrix, and with a decrease in α, the agglomeration degree of CNTs increases. The parameter, β, represents the volume ratio of dispersed CNTs in inclusions to the total volume of the CNTs. When $\beta = 1$, all the CNTs are located in the sphere areas. In the case of uniform dispersion of all CNTs, $\alpha = \beta$. When $\beta > \alpha$, a higher value of β illustrates less uniform dispersion of CNTs. The average volume fraction, $\nu_{\rm CNT}$, of CNTs in the composite is:

$$\nu_{\rm CNT} = \frac{V_{\rm CNT}}{V}. \tag{19}$$

Using Eqs. (17)-(19), the volume fractions of CNTs in the inclusions and in the matrix can be indicated as:

$$\frac{V_{\rm CNT}^{\rm inclusion}}{V_{\rm inclusion}} = \frac{\nu_{\rm CNT}\beta}{\alpha}, \frac{V_{\rm CNT}^{m}}{V - V_{\rm inclusion}} = \frac{\nu_{\rm CNT}\Big(1-\beta\Big)}{1-\alpha}. \tag{20}$$

In the first step, the effective elastic stiffness of the inclusions and the CNTs reinforced matrix were estimated, and in the second step, the overall property of the whole composite system, consisting of inclusions and polymer matrix reinforced with uniformly

dispersed CNTs, was calculated. The Mori-Tanaka method, based on the presented interphase model, was used in both steps. In the case of complete agglomeration of CNTs, all CNTs were considered in the inclusions, i.e. $\beta = 1$. Therefore, the local volume fraction of CNTs in the inclusions can be expressed as:

$$\frac{V_{\text{CNT}}}{V_{\text{inclusion}}} = \frac{\nu_{\text{CNT}}}{\alpha}. \tag{21}$$

4.2. Exfoliation and overlap of CNTs

Two parameters of overlap and exfoliation of CNTs have important influences on the final strength of the nanocomposite, which are not considered in classical micromechanics models. A finite element model was developed to analyze the effect of overlap and exfoliation of CNTs. The microstructure for the finite element model was simplified by assuming the CNTs as square, perfectly bonded to an interphase and parallel to each other. Figure 3 shows the microstructure model. To quantify the degree of CNT overlap, an overlap factor f_0 was introduced as [44]:

$$f_o = \frac{2 \times \text{offset}}{\text{B}}, \tag{22}$$

where B and offset are shown in Figure 3.

An overlap factor of $f_o = 0$ indicates that all CNTs are in perfect columns. Exfoliation is the other parameter related to CNT interaction. To control the level of exfoliation in the finite element model, exfoliation factor, f_x, was introduced as:

$$f_x = \frac{h}{h_{\max}} = \frac{L^2}{B^2}, \tag{23}$$

where:

$$h_{\max} = \frac{t}{\nu_{\text{CNT}}} \quad \text{and} \quad \nu_{\text{CNT}} = \frac{L^2 t}{B^2 h}. \tag{24}$$

An exfoliation factor of $f_x = 1$ illustrates the theoretical maximum exfoliation, though a smaller exfoliation factor indicates closer CNT spacing and greater gaps between CNT columns. The elastic properties of the interphase were assumed as previously calculated.

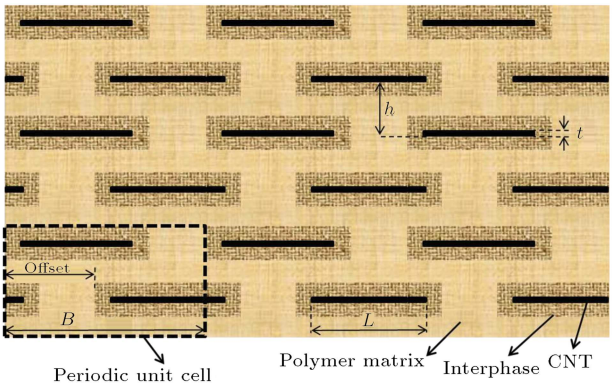

Figure 3. A schematic of microstructure model for finite element modeling.

Two-dimensional finite element models were developed for aligned oriented CNTs. In all models, the matrix and interphase were assumed isotropic and the CNTs transversely isotropic and linearly elastic. The finite element calculations were conducted using the commercial software, Abaqus. The four-node plane stress elements with reduced integration (CPS4R) were selected for CNTs, interphase and matrix. As the repeated unit cells represent a continuous physical body, two conditions need to be satisfied at the boundaries of the adjacent unit cells. Firstly, the neighboring unit cells should not be separated or break into each other at the boundaries after deformation. Therefore, the displacement field must be continuous. Secondly, the traction distributions at the opposite parallel boundaries of a unit cell must be the same. These conditions can be defined by applying the boundary condition called "Tie" in the interaction module of Abaqus software.

To determine the longitudinal elastic modulus of nanocomposites (E_1), the RVE was axially loaded (i.e. parallel to CNT orientation). A uniform strain was applied to the rightside of the model by a rigid reference node on the edge, while the normal displacement of the left side was fixed. Symmetry requires all faces (sides in the case of 2D) of the RVE to remain plane. Therefore, normal displacement of the bottom side in the 2D RVE was fixed, which required the top side to remain plane (in our case of a 2D model: straight line) and parallel to the coordinate axes. The tangential displacements of all sides were unconstrained. The average stress was calculated by dividing the reaction force by the cross-sectional area of the RVE.

5. Results and discussion

5.1. Interphase properties

A (6,6) single-wall CNT was considered for this nanocomposite and was supposed straight, finite-length, and transversely isotropic. The material properties are tabulated in Table 1. *A* colorless polyimide, LaRC-CP2, was considered as polymer matrix in which CNTs were assumed uniformly dispersed. The Young's modulus and Poisson ratio of this material are 0.85 GPa and 0.4, respectively [45].

The modeling results of micromechanics theories

Table 1. Elastic properties of (6,6) single-wall CNT [16].

E_{11} (GPa)	$E_{22} = E_{33}$ (GPa)	$G_{12} = G_{13}$ (GPa)	G_{23} (GPa)	$\nu_{12} = \nu_{13}$	ν_{23}
1220	19.77	36.17	7.32	0.2	0.35

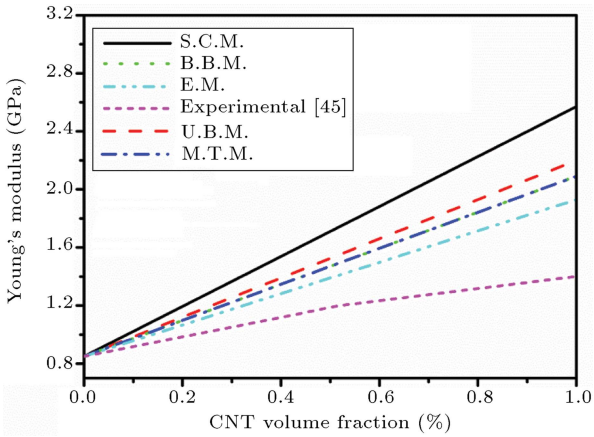

Figure 4. Comparison of classical micromechanics with experimental results.

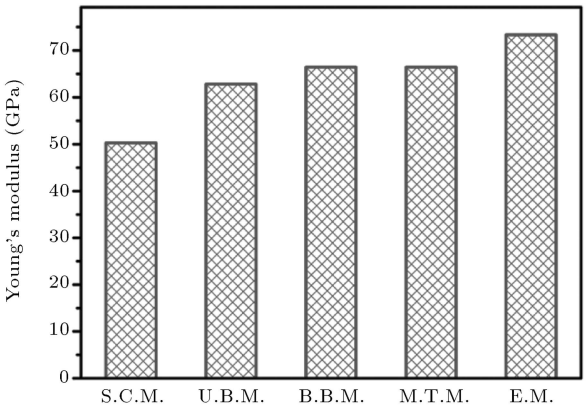

Figure 5. Young's modulus of the inclusion consisting of CNT and interphase.

for the SWCNT with a length of 3000 nm and various volume fractions are compared with experimental results [46] in Figure 4. In this figure, S.C.M. stands for Self-Consistent Model, U.B.M. for the Upper Bound of the Bounding Model, B.B.M. for the lower Bound of the Bounding Model, M.T.M. for the Mori-Tanaka Model and E.M. for the Eshelby Model.

A difference in the Young's modulus predicted using the classical micromechanics theories and experimental data was observed. The difference varied from about 16% at 0.5% volume fraction of CNT in the case of the Eshelby model to about 50% in the case of the self consistent model. Also, the theoretical predictions were higher than the experimental data, especially for values of CNT volume fraction greater than 0.5%. For example, at 1% nanotube volume fraction, the predicted Young's modulus by the Mori-Tanaka model was 2.09 GPa, which was 49% higher than the measured values from experiment. The difference between the experimental and theoretical results was most likely due to not considering the interphase by classical micromechanics theories. To solve this problem, an inclusion consisting of CNT and interphase was considered as the reinforcing constituent in the matrix. However, the Young's modulus of this inclusion is unknown and cannot be calculated because the modulus of the interphase is unknown. Using our presented two-step semi-analytical method, the Young's modulus of this inclusion was determined, such that the Young's modulus of the nanocomposite (consisting of this inclusion and matrix) predicted by each theory matches the experimental data. Figure 5 shows the calculated Young's modulus of the inclusion for each theory so that they can predict the same Young's modulus of nanocomposites as the experimental data. For example, in order to have the Young's modulus of nanocomposites predicted by SCM exactly the same as the experimental result, the Young's modulus of inclusion (CNT and matrix) should be considered around 50 GPa. Looking at Figure 4, we can see that SCM predicts the highest modulus for the nanocomposite, among all other theories, compared to the experimental result. Therefore, to predict the same Young's modulus for nanocomposite as the experimental result, the Young's modulus of the inclusion for this model should be the lowest value. Similarly, the Young's modulus of the inclusion for EM in Figure 5, which predicted the lowest nanocomposite modulus among all theories, is the highest, so that it can predict the same Young's modulus as experimental data. Using this method, the effects of micro-structural parameters on the overall mechanical properties of nanocomposites were investigated.

5.2. Effect of micro-structural parameters on elastic modulus of nanocomposites with aligned CNTs using the interphase model

In this section, the effect of microstructural parameters on elastic properties of the nanocomposite with aligned CNTs is studied using the interphase model. The prediction of the various micromechanics theories for the longitudinal Young's modulus of the aligned nanocomposite, as a function of CNT volume fraction for CNT aspect ratio of 100, is shown in Figure 6. In this figure, V.M. stands for Voigt Model, S.C.M. for Self-Consistent Model, U.B.M. for Upper Bound of Bounding Model, B.B.M. for lower Bound of Bounding Model, M.T.M. for Mori-Tanaka Model, E.M. for Eshelby Model, H.T.M. for Halpin-Tsai Model and R.M. for Reuss Model. It can be seen that Young's modulus increases with an increase in volume fraction. Bounding models, Mori-Tanaka and Eshelby models predict similar and close behavior for the nanocomposite. The Voigt model predicts the highest modulus and Reuss the lowest modulus for the nanocomposite. According to the Mori-Tanaka model, the longitudinal Young's modulus of the nanocomposite with 5% CNT volume fraction is 16.73 times larger than un-reinforced polymer.

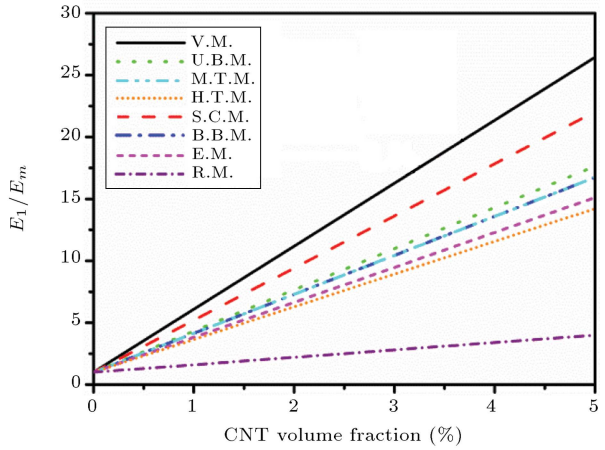

Figure 6. Longitudinal Young's modulus of a nanocomposite with aligned CNTs vs. CNT volume fraction using the interphase model.

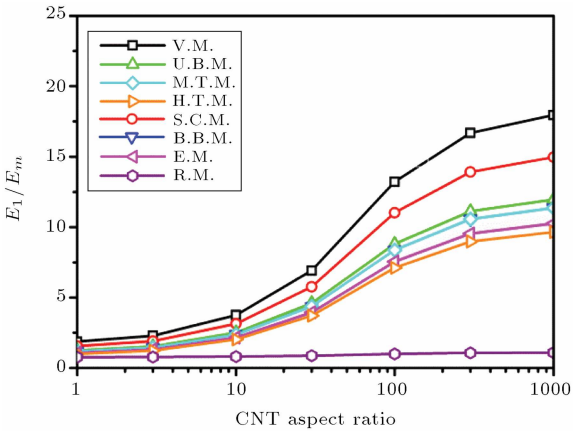

Figure 7. Longitudinal Young's modulus of a nanocomposite with aligned CNTs vs. CNT aspect ratio.

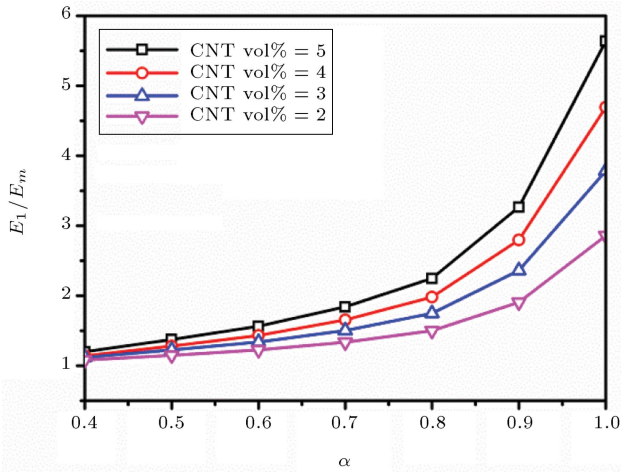

Figure 8. Effect of CNT agglomeration on the effective elastic modulus ($\beta = 1$).

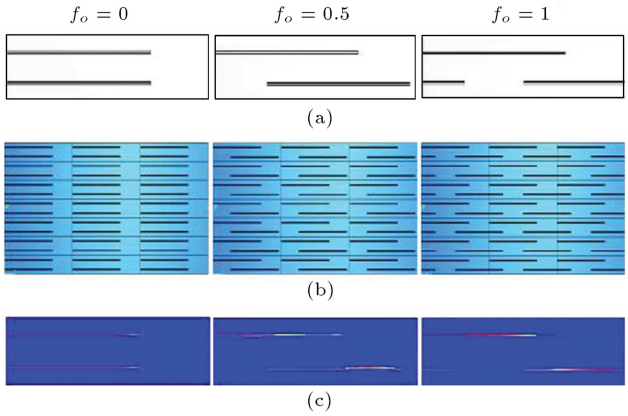

Figure 9. The FEM model for various staggering factors: (a) Unit cell; (b) assembled model; and (c) and longitudinal stress distribution.

Figure 7 is a plot of the calculated longitudinal Young's modulus for the aligned nanocomposite as a function of CNT aspect ratio. A significant increase in the slope of the Young's modulus curves occurs between CNT aspect ratio of 10 to 100. Both Mori-Tanaka and lower boundary models have similar predictions.

The Young's modulus, with respect to the agglomeration parameter α under different volume fractions of CNTs, is presented in Figure 8. When the CNTs are uniformly dispersed in the composite, i.e., $\alpha = 1$, the effective Young's modulus has maximum value. With a decrease in the agglomeration parameter, α, the stiffness decreases very rapidly. When $\alpha < 0.6$, increasing the CNTs volume fraction does not have an important effect on stiffening.

The model for three overlap factors and stress distribution around CNTs in a unit cell with a constant exfoliation factor is shown in Figure 9. A significant stress concentration can be seen on the ends of the CNTs in the unit cell with the highest CNT overlap ($f_o = 0$), which can result in the pull out of CNTs or cracking in the matrix. However, this stress concentration has been disappeared in the unit cells by a decrease in CNT overlap (increasing the overlap factor, f_o, from 0 to 0.5 and 1). Moreover, a more uniform stress distribution can be seen on the unit cells with a lower CNT overlap (a higher f_o).

Figure 10 illustrates stress distribution around the CNT in a unit cell with constant overlap factors and three exfoliation factors, 0.3, 0.5, and 0.7, in which horizontal distances between CNT ends are 412.87, 207.1 and 149.4, respectively.

The effect of overlap and exfoliation on the nanocomposite modulus is shown in Figure 11. The elastic modulus increases with an increase in overlap factor. In other words, a decrease in CNTs' overlap, leads to an increase in elastic modulus that may be due to better stress distribution in the CNTs and matrix. A decrease in the exfoliation factor, leads to a decrease in elastic modulus. Therefore, the modulus decreases with an increase in horizontal distance between the ends of the CNTs. It should be noted that an increase

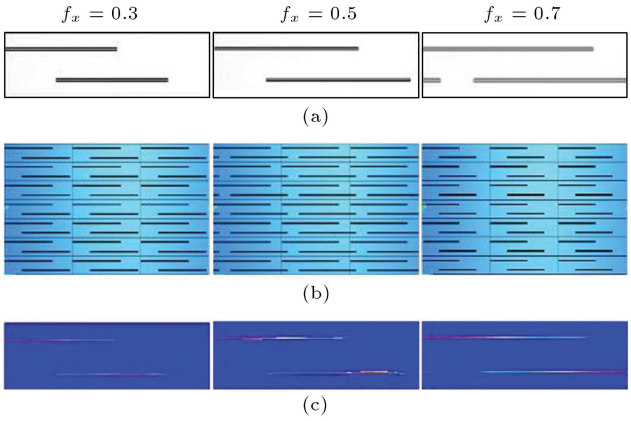

Figure 10. The FEM model for various exfoliation factors: (a) Unit cell; (b) assembled model; and (c) and longitudinal stress distribution.

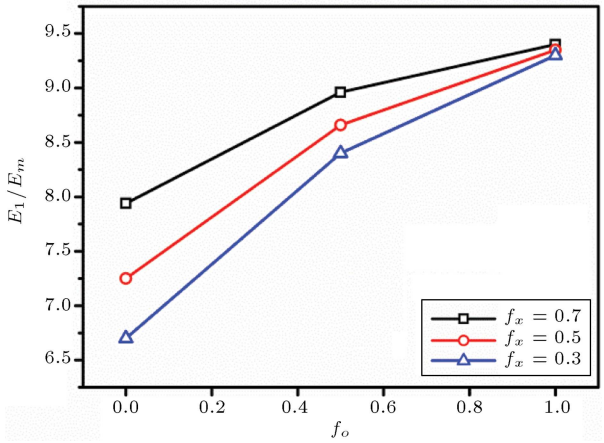

Figure 11. Dependency of modulus on overlap factor for various exfoliation factors.

in the exfoliation level, decreases the effect of the overlap factor on the elastic modulus.

6. Conclusions

In this study, the predictions of Young's modulus of nanocomposite, using classical micromechanics theories based on continuum mechanics, were evaluated and compared with experimental data. The result revealed a considerable difference between the predicted and experimental results, due to neglecting the interaction between CNTs and the polymer matrix in these theories. A model was developed to take into account the interphase effects for the exact prediction of nanocomposite Young's modulus. The effect of microstructural parameters on the nanocomposite Young's modulus was investigated using the presented method. The effect of agglomeration of CNTs on the Young's modulus of nanocomposites was examined, and the results showed that the maximum Young's modulus of nanocomposite can be achieved with uniform distribution of CNTs within the matrix. The effects of exfoliation and overlap of CNTs on the elastic properties of the nanocomposites were also studied using a finite element model. It was shown that the elastic modulus is increased with a decrease in CNT overlap and an increase in the exfoliation factor.

References

1. Nouri, N. and Ziaei-Rad, S. "Mechanical property evaluation of carbon nanotube sheets", *Scientia Iranica*, **17**(F2), pp. 90-101 (2010).
2. Yousefzadeh, M., Amani-Tehran, M., Latifi, M. and Ramakrishan, S. "Morphology and mechanical properties of polyacrylonitrile/multi-walled carbon nanotube (PAN/MWNTS) nanocomposite electrospun nanofibers", *Scientia Iranica*, **17**(F1), pp. 60-65 (2010).
3. Liu, Y.J., Nishimura, N., Qian, D., Adachi, N., Otani, Y. and Mokashi, V. "A boundary element method for the analysis of CNT/polymer composites with a cohesive interface model based on molecular dynamics", *Engineering Analysis with Boundary Elements*, **32**(4), pp. 299-308 (2008).
4. Frankland, S.J.V., Harik, V.M., Odegard, G.M., Brenner, D.W. and Gates, T.S. "The stress-strain behavior of polymer-nanotube composites from molecular dynamics simulation", *Composites Science and Technology*, **63**(11), pp. 1655-1661 (2003).
5. Haque, A. and Ramasetty, A. "Theoretical study of stress transfer in carbon nanotube reinforced polymer matrix composites", *Composite Structures*, **71**(1), pp. 68-77 (2005).
6. Pantano, A., Modica, G. and Cappello, F. "Multiwalled carbon nanotube reinforced polymer composites", *Materials Science and Engineering A*, **486**(1-2), pp. 222-227 (2008).
7. Ashrafi, B. and Hubert, P. "Modeling the elastic properties of carbon nanotube array/polymer composites", *Composites Science and Technology*, **66**(3-4), pp. 387-396 (2006).
8. Wan, H., Delale, F. and Shen, L. "Effect of CNT length and CNT-matrix interphase in carbon nanotube (CNT) reinforced romposites", *Mechanics Research Communications*, **32**(5), pp. 481-489 (2005).
9. Bradshaw, R.D., Fisher, F.T. and Brinson, L.C. "Fiber waviness in nanotube-reinforced polymer composites-ii: modeling via numerical approximation of the dilute strain concentration tensor", *Composites Science and Technology*, **63**(11), pp. 1705-1722 (2003).
10. Bafekrpour, E., Simon, G.P., Yang, C., Habsuda, J., Naebe, M. and Fox, B. "Effect of compositionalgradient on thermal behavior of synthetic graphite-phenolic

nanocomposites", *Journal of Thermal Analysis and Calorimetry*, **109**(3), pp. 1169-76 (2012).

11. Yas, M.H. and Heshmati, M. "Dynamic analysis of functionally graded nanocomposite beams reinforced by randomly oriented carbon nanotube under the action of moving load", *Applied Mathematical Modelling*, **36**(4), pp. 1371-1394 (2012).

12. Heshmati, M. and Yas, M.H. "Dynamic analysis of functionally graded multi-walled carbon nanotube-polystyrene nanocomposite beams subjected to multi-moving loads", *Materials and Design*, **49**, pp. 894-904 (2013).

13. Bafekrpour, E., Simon, G.P., Habsuda, J., Naebe, M., Yang, C. and Fox, B. "Fabrication and characterization of functionally graded synthetic graphite/phenolic nanocomposites", *Materials Science and Engineering A*, **545**, pp. 123-131 (2012).

14. Yas, M.H., Pourasghar, A., Kamarian, S. and Heshmatia, M. "Three-dimensional free vibration analysis of functionally graded nanocomposite cylindrical panels reinforced by carbon nanotube", *Materials and Design*, **49**, pp. 583-590 (2013).

15. Bafekrpour, E., Simon, G.P., Yang, C., Chipara, M., Habsuda, J. and Fox, B. "A novel carbon nanofibre/phenolic nanocomposite coated polymer system for tailoring thermal behaviour", *Composites Part A: Applied Science and Manufacturing*, **46**(1), pp. 80-88 (2013).

16. Odegard, G.M., Gates, T.S., Wise, K.E., Park, C. and Siochi, E.J. "Constitutive modeling of nanotube-reinforced polymer composites", *Composites Science and Technology*, **63**(11), pp. 1671-1687 (2003).

17. Huang, J. and Rodrigue, D. "Equivalent continuum models of carbon nanotube reinforced polypropylene composites", *Materials & Design*. **50**(0), pp. 936-945 (2013).

18. Shokrieh, M.M. and Rafiee, R. "On the tensile behavior of an embedded carbon nanotube in polymer matrix with non-bonded interphase region", *Composite Structures*, **92**(3), pp. 647-652 (2010).

19. Shokrieh, M.M. and Rafiee, R. "Prediction of mechanical properties of an embedded carbon nanotube in polymer matrix based on developing an equivalent long fiber", *Mechanics Research Communications*, **37**(2), pp. 235-240 (2010).

20. Yang, S., Yu, S., Ryu, J., Cho, J.M., Kyoung, W., Han, D.S. and Cho, M. "Nonlinear multiscale modeling approach to characterize elastoplastic behavior of CNT/polymer nanocomposites considering the interphase and interfacial imperfection", *International Journal of Plasticity*, **41**(0), pp. 124-146 (2013).

21. Eshelby, J.D. "The determination of the elastic field of an ellipsoidal inclusion, and related problems", *Proceedings of the Royal Society of London Series a-Mathematical and Physical Sciences*, **241**(1226), pp. 376-396 (1957).

22. Mori, T. and Tanaka, K. "Average stress in matrix and average elastic energy of materials with misfitting inclusions", *Acta Metallurgica*, **21**(5), pp. 571-574 (1973).

23. Hill, R. "A self-consistent mechanics of composite materials", *Journal of the Mechanics and Physics of Solids*, **13**(4), pp. 213-222 (1965).

24. Budians, K.B. "On elastic moduli of some heterogeneous materials", *Journal of the Mechanics and Physics of Solids*, **13**(4), pp. 223-227 (1965).

25. Halpin, J.C. "Stiffness and expansion estimates for oriented short fiber composites", *Journal of Composite Materials*, **3**, pp. 732-734 (1969).

26. Tucker, C.L. and Liang, E. "Stiffness predictions for unidirectional short-fiber composites: Review and evaluation", *Composites Science and Technology*, **59**(5), pp. 655-671 (1999).

27. Li, K., Gao, X.L. and Roy, A.K. "Micromechanical modeling of viscoelastic properties of carbon nanotube-reinforced polymer composites", *Mechanics of Advanced Materials and Structures*, **13**(4), pp. 317-328 (2006).

28. Narh, K.A., Jallo, L. and Rhee, K.Y. "The effect of carbon nanotube agglomeration on the thermal and mechanical properties of polyethylene oxide", *Polymer Composites*, **29**(7), pp. 809-817 (2008).

29. Shi, D.L., Feng, X.Q., Huang, Y.G.Y., Hwang, K.C. and Gao, H.J. "The effect of nanotube waviness and agglomeration on the elastic property of carbon nanotube-reinforced composites", *Journal of Engineering Materials and Technology - Transactions of the ASME*, **126**(3), pp. 250-257 (2004).

30. Weng, G. "Explicit evaluation of Willis' bounds with ellipsoidal inclusions", *International Journal of Engineering Science*, **30**(1), pp. 83-92 (1992).

31. Halpin, J.C. and Kardos, J. "The Halpin-Tsai equations: A review", *Polym. Eng. Sci*, **16**(5), pp. 344-352 (1976).

32. Marzari, N. and Ferrari, M. "Textural and micromorphological effects on the overall elastic response of macroscopically anisotropic composites", *Journal of Applied Mechanics*, **59**, pp. 269 (1992).

33. Liu, T.X., Liu, Z.H., Ma, K.X., Shen, L., Zeng, K.Y. and He, C.B. "Morphology, thermal and mechanical behavior of polyamide 6/layered-silicate nanocomposites", *Composites Science and Technology*, **63**(3-4), pp. 331-337

34. Odegard, G.M., Clancy, T.C. and Gates, T.S. "Modeling of the mechanical properties of nanoparticle/polymer composites", *Polymer*, **46**(2), pp. 553-562 (2005).

35. Bafekrpour, E., Simon, G.P., Yang, C., Habsuda, J., Naebe, M. and Fox, B. "Effect of compositional gradi-

ent on transient temperature field in carbon nanofiber-phenolic nanocomposites", *in NANOSMAT*, Tampa, USA (2012).

36. Jam, J.E., Pourasghar, A., Kamarian, S. and Maleki, S. "Characterizing elastic properties of carbon nanotube-based composites by using an equivalent fiber", *Polymer Composites*, **34**(2), pp. 241-251 (2013).
37. Shokrieh, M.M. and Rafiee, R. "Development of a full range multi-scale model to obtain elastic properties of CNT/polymer composites", *Iranian Polymer Journal* (English Edition), **21**(6), pp. 397-402 (2012).
38. Stephan, C., Nguyen, T., de la Chapelle, M.L., Lefrant, S., Journet, C. and Bernier, P. "Characterization of singlewalled carbon nanotubes-pmma composites", *Synthetic Metals*, **108**(2), pp. 139-149 (2000).
39. Bafekrpour, E., Simon, G.P., Naebe, M., Habsuda, J., Yang, C. and Fox, B. "Preparation and properties of composition-controlled carbon nanofiber/phenolic nanocomposites", *Composites Part B: Engineering*, **52**, pp. 120-126 (2013).
40. Bafekrpour, E., Simon, G.P., Naebe, M., Habsuda, J., Yang, C. and Fox, B. "Composition-optimized synthetic graphite/polymer nanocomposites", *in NPE-ANTEC*, Orlando, USA pp. 437-441 (2012).
41. Bafekrpour, E., Yang, C., Natali, M. and Fox, B. "Functionally graded carbon nanofiber/phenolic nanocomposites and their mechanical properties", *Composites Part A: Applied Science and Manufacturing*, **54**, pp. 124-34 (2013).
42. Bafekrpour, E., Simon, G.P., Yang, C., Chipara, M., Habsuda, J. and Fox, B. "Functionally graded carbon nanofiber-phenolic nanocomposites for sudden temperature change applications", *Polymer*, **54**(15), pp. 3940-8 (2013).
43. Bafekrpour, E., Yang, C., Natali, M. and Fox, B. "Functionally graded carbon nanofiber/phenolic nanocomposites and their mechanical properties", *Composites Part A: Applied Science and Manufacturing*, **54**, pp. 124-34 (2013).
44. Fertig III, R.S. and Garnich, M.R. "Influence of constituent properties and microstructural parameters on the tensile modulus of a polymer/clay nanocomposite", *Composites Science and Technology*, **64**(16), pp. 2577-2588 (2004).
45. Thompson, C. "Preparation and characterization of metal oxide/polyimide nanocomposites", *Composites Science and Technology*, **63**(11), pp. 1591-1598 (2003).
46. Park, C., Ounaies, Z., Watson, K.A., Crooks, R.E. and Smith, J. "Dispersion of single wall carbon nanotubes by in situ polymerization under sonication", *Chemical Physics Letters*, **364**(3-4), pp. 303-308 (2002).
47. Tandon, G. and Weng, G. "Average stress in the matrix and effective moduli of randomly oriented composites", *Composites Science and Technology*, **27**(2), pp. 111-132 (1986).

Appendix

The components of Eshelby's tensor, H_{ijkl}, are [47]:

$$H_{1111} = \frac{1}{2(1-\nu_m)}\left\{1-2\nu_m+\frac{3(l/d)^2-1}{(l/d)^2-1} - \left[1-2\nu_m+\frac{3(l/d)^2}{(l/d)^2-1}\right]g\right\}$$

$$H_{2222} = H_{3333} = \frac{3}{8(1-\nu_m)}\frac{(l/d)^2}{(l/d)^2-1}+\frac{1}{4(1-\nu_m)}\left[1-2\nu_m-\frac{9}{4\left((l/d)^2-1\right)}\right]g$$

$$H_{2233} = H_{3322} = \frac{1}{4(1-\nu_m)}\left\{\frac{(l/d)^2}{2\left((l/d)^2-1\right)} - \left[1-2\nu_m+\frac{3}{4\left((l/d)^2-1\right)}\right]g\right\}$$

$$H_{2211} = H_{3311} = -\frac{1}{2(1-\nu_m)}\frac{(l/d)^2}{(l/d)^2-1}+\frac{1}{4(1-\nu_m)}\left[\frac{3(l/d)^2}{(l/d)^2-1}-(1-2\nu_m)\right]g$$

$$H_{1122} = H_{1133} = -\frac{1}{2(1-\nu_m)}\left[1-2\nu_m+\frac{1}{(l/d)^2-1}\right] + \frac{1}{2(1-\nu_m)}\left[1-2\nu_m+\frac{3}{2\left((l/d)^2-1\right)}\right]g$$

$$H_{2323} = H_{3232} = \frac{1}{4(1-\nu_m)}\left\{\frac{(l/d)^2}{2\left((l/d)^2-1\right)} - \left[1-2\nu_m-\frac{3}{4\left((l/d)^2-1\right)}\right]g\right\}$$

$$H_{1212} = H_{1313} = \frac{1}{4(1-\nu_m)}\left\{1-2\nu_m-\frac{(l/d)^2+1}{(l/d)^2-1} - \frac{1}{2}\left[1-2\nu_m-\frac{3\left((l/d)^2+1\right)}{(l/d)^2-1}\right]g\right\},$$

where g is given by:

$$g = \frac{(l/d)}{\left(1-(l/d)^2\right)^{3/2}}\left[\cos^{-1}\alpha-\alpha\left(1-(l/d)^2\right)^{1/2}\right]$$

Biographies

Ehsan Bafekrpour obtained a BS degree in Me-

chanical Engineering (solid mechanics) from Babol Noshirvani University of Technology, Iran, an MS degree in Mechanical Engineering (applied design) from Amirkabir University of Technology, Iran, and a PhD degree from Deakin University, Australia. He is currently a Research Fellow at the Centre for Advanced Hybrid Materials, Department of Materials Engineering, Monash University, Australia. His research interests include advanced hybrid and composite materials, functionally graded materials, numerical and analytical modelling, and experimental material characterizations.

Manouchehr Salehi completed his BS degree (Hons) in Production Engineering, in 1984, his MPhil in Mechanical Engineering, in 1987, at Leeds Metropolitan University, UK, and his PhD degree, in 1990, from Lancaster University, UK, where he undertook a comprehensive research program on numerical and experimental analysis of stiffened and unstiffened sector plates. He is currently Associate Professor in Solid Mechanics in the Mechanical Engineering Department of Amirkabir University of Technology, Tehran, Iran. Dr Salehi has presented fifty papers at international and national conferences, has more than thirty referred journal publications and has authored a book on 'Optimization of Composite Structures using Genetic Algorithm.

Ehsan Sonbolestan received a BS degree from the Department of Engineering at the University of Shahrekord, Iran, in 2003, and an MS degree from the Department of Mechanical Engineering at Iran University of Science & Technology (IUST), in 2005. He is currently a lead mechanical engineer in the Mapna Company, Iran (an oil and gas consulting company). His research interests include industrial applications and mechanical macro properties of various types of nanocomposites.

B. Fox. His/her biography was not available at the time of publication.